Songklanakarin J. Sci. Technol.
44 (6), 1434-1441, Nov. – Dec. 2022

http://www.sjst.psu.ac.th

Original Article

Anomaly detection in geostatistical models with application to groundwater level data in the Gaza Coastal Aquifer

Ali H. Abuzaid[1*], Diana A. Aish[1], and Maroua Benghoul[2]

[1] *Department of Mathematics, Faculty of Science, Al Azhar University-Gaza, Gaza, Palestine*

[2] *Department of Statistics, Anadolu University, Eskişehir, Turkey*

Received: 22 June 2022; Revised: 26 August 2022; Accepted: 13 October 2022

Abstract

In geostatistics, the detection of anomalous observations has a particular importance because of the changes they can create in environmental and geological patterns. Few methods for detecting such observations in univariate data have been proposed for the spatial case, namely sample influence function (SIF), kriging, Intrinsic Random Functions (IRF), and geostatistical functional data. This article reviews the main outlier detection procedures in the context of geostatistics, and due to the absence of a numerical comparison between them, this article obtained the cut-off points of these methods for three different variogram models, and evaluated their performance via a simulation study. The results show that for all detection methods and the three considered models, there is an inverse relationship between the level of contamination and power of performance. In addition, the SIF for the cubic variogram model outperforms the exponential and Matérn. Because of the peculiarities of the Gaza Strip, as regards Palestine water condition, and for illustration purposes, we consider real groundwater level data in the Gaza Coastal Aquifer, where a set of possible outliers were identified.

Keywords: geostatistics, variogram, kriging, sample influence function, intrinsic random functions, R

1. Introduction

Geostatistics is a branch of statistics that describes the spatial continuity of natural phenomena (Isaaks, & Srivastava, 1989). It collects theories and numerical techniques to deal with the characterization of spatial attributes, by employing primarily random models in a similar way as temporal data is characterized in time series analysis (Olea, 2012).

Geostatistics has many applications in different fields, for instance in modeling groundwater management (Ahmed, 2007) or in COVID-19 prevalence maps (Azevedo, Pereira, Ribeiro, & Soares, 2020), analyses of the spatial patterns of physical or chemical attributes of soil (Sun *et al.*, 2022), or the estimation of contaminant levels in environment (Gilbert, & Simpson, 1985).

*Corresponding author
Email address: a.abuzaid@alazhar.edu.ps

The unusual readings known as outliers or anomalous data on groundwater level may lead to serious inferential statistical problems, including the misspecification of the best model as well as poor prediction of further readings. Outlier in the context of geostatistics may be defined as any features in locations that are abnormally isolated compared to the neighboring values.

Geostatistical data analysis is sensitive to outliers and there are only few proposed outlier detection procedures, based on certain characteristics of geostatistical methods as reviewed in Section 2.

Nirel Mugglestone and Barnett (1998) suggested a method for eliminating spatial data that involves detecting outliers first, then replacing them with values calculated from the remaining data. Yoo and Um (1999) developed two alternative strategies for detecting spatial outliers**:** the distributional inference method and the deletion method. Kim and Jung (2005) proposed the outlier detection method using multivariate regression based on the sign of the influence function. Hayashi, Ishioka, Ueda, Suito, and Kurihara (2013)

proposed a new framework of statistical sensitivity analysis for linear discriminant analysis. Kim (2014) discussed an estimation approach based on maximum likelihood method, and detected outliers with the sample influence function.

The Gaza Strip is a narrow area lying along the south-eastern coast of the Mediterranean Sea in the southwestern part of Palestine between 34° 2′ and 34° 25′ east longitudes and 31° 16′ and 31° 45′ north latitudes. Gaza Strip is especially sensitive to the effects of climate change due to its dense population, dry environment, and water scarcity challenges. Furthermore, the coastal aquifer is the primary supply of freshwater. According to recent estimates, 97% of the water in the Gaza Strip's Coastal Aquifer is already unsuitable for human use, and the damage to the Aquifer is expected to be permanent if prompt action is not taken (United Nations Children's Fund [UNICEF], 2018).

There hasn't been any research comparing the performance of outlier detection methods in geostatistical data. Thus, this article investigates and compares the univariate outlier detection procedures via an extensive simulation study and applies them to the groundwater level data in the Gaza coastal aquifer.

The rest of this article is organized as follows. Section 2 presents outlier detection methods for geostatistical data. Section 3 obtains the cut-off points for the studied methods and compares their performance via an extensive simulation study. Section 4 applies outlier detection methods to real groundwater level data for the Gaza Coastal Aquifer.

2. Outlier Detection Methods

The basic components of geostatistics are variogram analysis, Kriging, and map interpolation, as explained in (Abuzaid, 2018).

Variogram is a measure of spatial correlation, or alternatively the variation between successive points, and it is obtained as follows.

$$h(\vec{\gamma}) = \frac{1}{2}E\left[\left[Z(\vec{x}+\vec{h})-Z(\vec{x})\right]^2\right] = \frac{1}{2}Var\left[\left[Z(\vec{x}+\vec{h})-Z(\vec{x})\right]^2\right],$$

where $Z(\vec{x})$ and $Z(\vec{x}+\vec{h})$ are random variables, $\vec{x}$ and $\vec{x}+\vec{h}$ are the spatial positions separated by a vector $\vec{h}$. The $h(\vec{\gamma})$ depends only on the separation vector $\vec{h}$ but not on the location $\vec{x}$.

Kriging is a tool of spatial prediction to estimate unknown local values of variables that are distributed in a space of finite dimension. It attempts to model the variability in the data as a function through the variogram (Isah, 2009). In Kriging each observation is given a weight according to the direction and distance between that point and the point to be estimated (Vieira., Hartfield, Nielsen, & Biggar, 1982).

There are six types of kriging used in geostatistical analysis, namely:

Ordinary Kriging (OK): The most used of kriging types. It assumes that the expected value is an unknown constant. $\hat{Z}(\vec{x}_0) = \sum_{i=1}^{n}\lambda_i Z(\vec{x}_i)$, where $Z(\vec{x}_i)$ is the measured value at ith location, λ_i are unknown weights for the measured values by location, $\vec{x}_0$ is predication location, and n is the number of measured values.

Simple Kriging (SK): This is the simple type, where the mean is known and constant over the domain, and the weights are not equal to 1, given by

$$\hat{Z}(\vec{x}_0) = \mu_0 + \sum_{i=1}^{n}\lambda_i(Z(\vec{x}_i)-\mu_0),$$

where $\sum_{i=1}^{n}\lambda_i$ is a constant c.

Universal Kriging (UK): This is different from the suppositions of ordinary and simple kriging, as the mean $\mu(\vec{x})$ is a linear combination of known functions at $\vec{x}$. It is defined as follows $\mu(\vec{x}) = \sum_{j=1}^{p}\beta_j f_j(\vec{x})$, where β_j are unknown coefficients of linear combination, $f_j(\vec{x})$ is a basic function of spatial coordinates that describes the drift, and p is the number of functions used in modeling the drift.

Block Kriging (BK): This is the mother of all forms of kriging for the characterization of a single attribute. It is reformulated of ordering kriging equations to estimate an average value $Z_V(\vec{x}_o)$ of the variable Z on a block of area v around $\vec{x}_0$, defined by

$$Z_v(\vec{x}_0) = \frac{1}{|v|}\int_v Z(\vec{x})\quad dx\ .$$

Co-Kriging (CK): This is basically a generalization of kriging. Co-kriging is a multivariate estimation procedure that contracts with two or more attributes within the same field. The best-unbiased predictor of $Z(\vec{x}_0)$ is estimated as a linear combination of both the variables of interest $Z(\vec{x})$ and the secondary variable $Y(\vec{x})$ and is given by

$$\hat{Z}(\vec{x}_0) = \sum_{i=1}^{n}\lambda_i Z(\vec{x}_i) + \sum_{j=1}^{m}\omega_j Y(\vec{x}_j)\ ,$$

where λ_i, ω_j are the weights and n, m are the numbers of a random variables.

Disjunctive Kriging (DK): It is the most complex way that makes it unappealing for most interested in this field. It is used to estimate the value of any function of the variable; however disjunctive kriging provides a solution space larger than other kriging techniques that only rely on non-linear combinations of the data.

For further characteristics of the previous types of kriging (Lichtenstern, 2013; Olea, 2012).

Spatial interpolation is the process of predicting unknown points based on a set of points with known values. There are many interpolation methods, where the most widely used interpolation method is Inverse Distance Weighting (IDW) which uses the values at known points during estimation of an unknown point, and the values known near the estimated site get larger weights than those far away: the weights will decrease with distance. Another method is the Triangulated Irregular Networks (TIN), which is one way to represent three-dimensional data for map interpolation. It depends on the point's location and the non-spatial data value necessary to create the three-dimensional coordinate surface and then connects them with lines that form triangles. The height can be calculated in any area and produces a network from triangles with irregular forms. For further explanation (Chang, 2006).

This section reviews four univariate geostatistical methods for detecting outliers, namely sample influence functions, kriging, intrinsic random functions, and geostatistical functional data.

2.1 Influence functions

An influence function is the effect of a specific observation on the estimator for an uncontaminated distribution. The Theoretical Influence Function (TIF) is defined as follows (Hampel, 1974)

$$TIF(Z(x),F) = \lim_{\varepsilon\to 0}\frac{T((1-\varepsilon)F+\varepsilon\delta_{Z(x)})-T(F)}{\varepsilon}, \quad (2.1)$$

where $T(F)$ is a parameter which can be considered as a functional of the cumulative distribution function F of random variables $Z(x)$ and $\delta_{Z(x)}$ is the cumulative distribution function. The Empirical Influence Function (EIF) is obtained by replacing cumulative distribution function F by $\widehat{F}$ in (2.1). The Sample Influence Function (SIF) is obtained by deleting *limit* and setting $\varepsilon = -\frac{1}{n-1}$, and it is expressed as:

$$SIF(Z(x_i),\hat{T}) = (n-1)[\hat{T}_i - \hat{T}]\ . \quad (2.2)$$

SIF is used to detect outliers based on their effect on the maximum likelihood estimate of the variogram model as follows (Kim, 2014)

$$SIF(De,\hat{L}) = \frac{n-t}{t}(\hat{L}_{De}-\hat{L})\ , \quad (2.3)$$

where n is the size of full data, t is the number of data in the subset to be evaluated (*De)*, $\hat{L}$ and $\hat{L}_{De}$ are the values of maximum log-likelihood of the considered variogram model for full data and reduced data, respectively. Alternatively, SIF could be used to detect outliers based on Akaike Information Criterion $AIC = 2(n-\hat{L})$, and is given by

$$SIF(De,AIC) = -\frac{n-t}{t}(AIC_{De}-AIC)\ . \quad (2.4)$$

where AIC_{De} is the AIC for the reduced sample. The largest absolute value of the SIF indicates possibility of outliers.

2.2 Kriging

Based on kriging, we can obtain the absolute value of the difference between the observed and the expected values, in relation to the variance of the estimation. This criterion is called the Absolute Normalized Deviation (AND), and formulated by:

$$\text{AND} = \frac{\hat{Z}(x_i)-Z(x_i)}{\sigma_i}\ , \quad (2.5)$$

where σ_i is the standard deviation of the estimation error.

If AND 's value for a given point is larger than three, then this point is an outlier. In addition AND is approximately normally distributed with a mean of zero and a variance of one (Cooper, & Istok, 1988). In order to apply plausibility analysis to structured data, it is necessary to calculate kriging variance. After selecting the type of variogram model and determining its parameters, we need to carry out validation for all data and test if the AND distribution is similar to the standard normal distribution *N*(0, 1). In that case, if the value of AND is higher than its maximum allowable value, then the point is an outlier.

2.3 Intrinsic random functions

The intrinsic random function (IRF) was developed as an alternative to universal kriging (Matheron, 1973). The IRF assumes that generalized increments of the observed random process lead to a second-order stationary process, while the universal kriging requires only that the mean structure of the observed process be linear, and between them there is great overlap, i.e., any polynomial universal kriging model with a stationary covariance function is an IRF (Delfiner, 1976).
The generalized polynomial covariances for IRF- *K* are defined as follows (Matheron, 1973):

$$K(h_{ij}) = c\delta(h) + \sum_{m=1}^{k}(-1)^{m+1}a_m h^{2m+1} \quad (2.6)$$

where $\delta(h)=1$ if $h=0$ and $\delta(h)=0$ elsewhere. The coefficients must satisfy some additional conditions, $c\geq 0, a_0\geq 0, a_2\geq 0$ and $a_1\geq 10\sqrt{a_0 a_2}/3$. This can be done in a variety of ways, including the weighted regression techniques (Delfiner, 1976), and the minimum norm estimator (Kitanidis, 1983).

Arrangements of IRF coefficients yielding the smallest deviations of AND features from the standard normal distribution. If the raw data cannot reach the acceptable value of the variance of AND, the observation point with the highest value of AND is characterized as an outlier and momentarily excluded from the results.

Due to the less straightforward theory of the IRF it is less commonly used than the AND kriging method (Bárdossy, & Kundzewicz, 1990).

2.4 Functional data

The functional data analysis (FDA) is a modern branch of statistics that analyzes data by providing information about curves, surfaces or anything else varying over a continuum. It is used to enhance, analyze, model and predict time series data (Giraldo, *et al.* 2011).

The spatial functional process is denoted by:

$$Z_{x_i}(t_j) = \mu_{x_i}(t_j) + \varepsilon_{x_j}(t_j), \quad (2.7)$$

where $\varepsilon_{x_j}(t_j)$ are residuals with independent zero mean, and $\mu_{x_i}(t_j)$ is the mean function which summarizes the main structure of Z_{x_i}.

$Z_{x_i}(t_j)$ is assumed to be second-order stationary and isotropic (i.e., the mean and variance functions are constant and the covariance depends only on the distance between points). Moreover, consider that for every fixed $t_0\in[a,b]$, the finite-dimensional section $Z_{x_i}(t_0)$ is a random function defined on some probability space.

The outliers in geostatistical functional data are defined as the curves spatial locations that are not compatible with their neighborhoods, which can be a lonely outlier or a group of outliers (Febrero, Galeano, & González-Manteiga, 2008).

Within the functional context, many depth functions are proposed, including the modal depth dependent on the definition of mode. The modal depth of the spatial function is defined as the curve that achieves the maximum value as follows (Cuevas, Febrero, & Fraiman, 2007):

$$SMD(Z_{x_i}(t)) = \sum_{j=1}^{n} K\left(\frac{\left\|Z_{x_i} - Z_{x_j}\right\|_w}{b}\right) \qquad (2.8)$$

where $K : \mathbb{R}^+ \to \mathbb{R}^+$ is a kernel function, b is a bandwidth parameter, and $\left\|Z_{x_i} - Z_{x_j}\right\|_W$ is the distance between the geo-referenced curves weighted by the spatial variation between the sites, and represented by:

$$d_w(Z_{x_i}, Z_{x_j}) = d(Z_{x_i}, Z_{x_j})\ \gamma_{ij}(h) \qquad (2.9)$$

where $d(Z_{x_i}, Z_{x_j}) = \sqrt{\int_T Z_{x_i}(t) - Z_{x_j}(t))^2 dt}$ is the distance between the curves without the spatial component. In general, the outliers of the spatial functional structure have $Pr(SMD(Z_{x_i}(t)) < \alpha) = 0.01$. The proportion of outliers then equals 1% (Romano and Mateu, 2013).

Since the theoretical distribution of SMD is not known, its empirical distribution is used to estimate the value of α based on bootstrap of the curves in the original set with a probability proportional to depth (Febrero, Galeano, & González-Manteiga, 2008).

No comparison study has been conducted to compare the performance of these methods. Since the nature of the SMD is different from the other detection methods, the following section will obtain the cut-off points for the first three outlier detection methods, namely SIF, AND and IRF, and compare their performance via a simulation.

3. Simulation Study

In order to compare the performance of detection methods, this section focuses on obtaining cut-off points for the three outlier detection methods SIF, AND and IRF in geostatistical data, and investigates their performances via a simulation study.

All required subroutines have been written by using (*sp*, *gstat*, *ggplot2*, *scales* and *geoR*) packages in R statistical environment, and are available upon request from the authors.

3.1 The cut-off points for geostatistical methods

The cut-off points for the three geostatistical methods, namely sample influence functions (SIF), kriging AND, and intrinsic random functions (IRF), are determined for three popular variogram models: exponential, cubic and Matérn variogram models. An unconditional simulation is designed for 7×7, 10×10, 15 ×15 and 20×20 sizes of grids without contamination of process, and with mean of W=3.

Under the null hypothesis the *i*th point is a consistent point (H_0: There is no outlier in the sample) while in the alternative hypothesis the *i*th point is an outlier (H_1: The *i*th point is outlier). For each combination of sample size *n* and variogram model, the process is repeated 1000 times to ensure the convergence of cut-off points. Then for each detection method the maximum value of statistics SIF, AND, and RIF are obtained, and 95% percentile of all obtained maximum value are determined to be considered as the cut-off (i.e. critical value) for the test statistic for every outlier detection. The cut-off points of the three considered outlier detection methods using exponential, cubic and Matérn variogram models are given in Table 1.

The cut-off points show an increase with sample size. Moreover, the SIF has the largest cut-off points among the detection methods, while the cubic variogram model has the largest values.

The following subsection investigates the performance of the three considered outlier-detection methods in geostatistical analysis.

3.2 Power of performance

The power of performance of discordancy tests can be evaluated by different methods (Barnett, & Lewis, 1994). The most common is the power of test $P1 = 1\text{-}\beta$, where β is the probability of Type-II error of the test.

Without loss of generality, the same generation approach as in the previous subsection is followed with respect to size, outlier-detection methods, and variogram models with mean W=3. For evaluating the performance, four levels of contamination (0%, 10%, 30% and 50%) are considered by generating the contaminated points from the same settings of the original data except that the mean was shifted to be $W_C = 8$.

Table 1. The cut-off points of the geostatistical methods

Method	Model	Size			
		7×7	10×10	15×15	20×20
SIF	Exp.	528.952	1175.502	3244.319	6110
	Cub.	665.602	1723.966	5806.276	12957.555
	Mat.	524.898	1225.874	3135.930	6243.293
AND	Exp.	6.536	8.391	13.453	23.489
	Cub.	23.224	70.643	103.429	186.734
	Mat.	6.740	12.664	19.311	23.694
IRF	Exp.	12.137	16.114	19.054	24.967
	Cub.	19.633	28.401	30.594	41.821
	Mat.	12.719	16.285	19.089	24.058

Then test statistics were obtained for each contaminated dataset, and compared with the associated cut-off point. The power of performances against the degrees of contamination are given in Table 2.

The performance of detection methods for small samples (7×7) is wobbly with respect to variogram models, contamination level or the detection methods. For the larger sample (10×10) and onwards the following behaviors are noticed.

For all detection methods and the three considered models, there is an inverse relationship between the level of contamination and power of performance.

AND kriging method has almost a constant performance for the three considered variogram models, with the weakest performance compared to the SIF and IRF. The performance of SIF for the cubic variogram model outperforms the exponential and Matérn.

4. Application to Groundwater Level Data in the Gaza Coastal Aquifer

The area of the Gaza Strip is about 365 km^2 with a length of 45 km and a width between 7 and 14 km (Aish, Ayesh, & Al-Najar, 2021). The Strip mainly is divided into five governorates: North Gaza, Gaza, Middle Governorate, Khanyounis and Rafah. The population density in the Gaza Strip is considered to be the highest in the world, with a population of more than 2 million people and a growth rate of about 3.5% annually (Palestinian Central Bureau of Statistics, [PCBS], 2020).

The Gaza aquifer is a major component of the water resources in the area. It is naturally recharged by precipitation and additional recharge occurs by irrigation return flow. Pumping wells (both municipal and agricultural wells) are the main internal hydrologic stresses acting on the Gaza aquifer system. According to (Palestinian Water Authority [PWA], 2010), about 4600 water wells across the Gaza Strip have been dug over the recent decades to meet both domestic and agricultural demands. The water consumption has increased substantially over the past years; the groundwater abstraction is about 187 M m^3 /year for the agricultural, industrial and domestic uses (PWA, 2015).

The water level data for the year 2019 were collected from Palestinian Water Authority (PWA), department of Hydrology. Groundwater level is monitored quarterly by (PWA) monitoring team, at 86 monitoring wells distributed spatially and covering the whole Gaza Strip area, as shown in Figure 1.

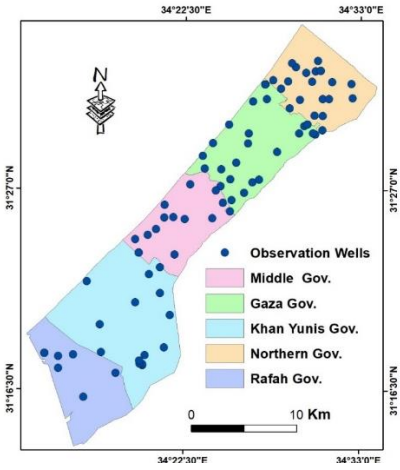

Figure 1. Location map and areal distribution of observation wells in the Gaza Strip

Table 2. The power of performance

Method	Model	Contamination level (7×7)			Contamination level (10×10)		
		10%	30%	50%	10%	30%	50%
SIF	Exp.	90.20%	0.0%	0.0%	38.19%	0%	0%
	Cub.	91.27%	80.48%	82.27%	97.45%	97.39%	97.81%
	Mat.	88.80%	0.0%	0.0%	29.14%	0%	0%
AND	Exp.	37.10%	32.33%	32.27%	18.56%	14.04%	14.18%
	Cub.	35.73%	32.33%	32.27%	15.91%	14.03%	14.19%
	Mat.	36.47%	32.32%	32.27%	14.97%	14.03%	14.18%
IRF	Exp.	64.1%	57.57%	44.69%	86.12%	70.05%	51.63%
	Cub.	75.23%	65.38%	54.77%	83.46%	65.84%	50.63%
	Mat.	63.95%	56.78%	43.43	86.01%	69.79%	51.29%
Method	Model	Contamination level (15×15)			Contamination level (20×20)		
		10%	30%	50%	10%	30%	50%
SIF	Exp.	70.78%	66.85%	57.24%	63.14%	60.25%	56.35%
	Cub.	73.68%	69.85%	60.15%	65.62%	62.95%	58.42%
	Mat.	69.54%	63.24%	52.84%	62.24%	58.64%	50.74%
AND	Exp.	35.07%	34.45%	34.74%	15.43%	15.56%	15.48%
	Cub.	34.87%	34.45%	34.74%	15.50%	15.56%	15.48%
	Mat.	34.95%	34.52%	34.68%	15.43%	15.56%	15.48%
IRF	Exp.	59.95%	43.85%	28.78%	80.82%	59.16%	41.56%
	Cub.	67.06%	51.66%	40.42%	73.48%	55.04%	40.35%
	Mat.	59.92%	43.77%	28.71%	82.75%	61.22%	43.26%

4.1 Data description

There are 86 observations in groundwater level data for the Gaza Coastal Aquifer. The values range between -20 m and 20.14 m, with mean and median -1.6711 and -2.6585 respectively, where the minus sign (-) indicates that the groundwater level is below the mean sea level (MSL). The box-plot in Figure 2 shows a set of outliers.

The groundwater level >5 meter above sea level is found in the eastern part of Rafah Governorate. The aquifer in that area is then a few meters, and not suitable for wells in the area. The PWA recorder maybe does not give attention to these observations and the wells have error in measurements assumptions, so these values are expected to be identified as outliers. Regarding groundwater level < -10 m, there are fluctuating water levels in the area due to excessive pumping causing differences and errors in measurement.

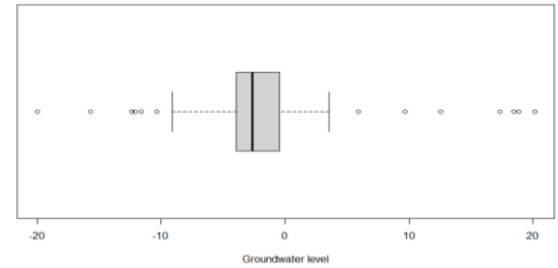

Figure 2. Box-plot of the groundwater level

4.2 Modeling and prediction

There are various variogram models that can be used for prediction. Table 3 shows three variogram models associated with cross-validation estimates of unknown groundwater levels in the Gaza Coastal Aquifer.

Table 3 shows that mean error (ME), mean squared error (MSE), and mean standardized squared error (MSSE) measures of exponential and Matérn variogram models are equal and smaller than for the cubic variogram measures. Thus, we select the exponential variogram model due to its simplicity. Consequently, the exponential variogram model (with nugget 0.80643, partial sill 64.5648 and range 13923.93) fitted to the empirical variogram was the best choice for modeling the spatial structures in the groundwater level data for the Gaza Coastal Aquifer.

Table 3. Cross-validation results of groundwater level modeling

Variogram model	ME	MSE	MSSE
Exponential	-0.0297546	7.45862	11.3919
Cubic	-0.222327	17.10928	25.98509
Matérn	-0.0297546	7.45862	11.3919

Following the selection of the best model, interpolated spatial distribution maps of these parameters are created. Figure 3 shows the ordinary kriging prediction of groundwater level distributed spatially into nine levels from very low groundwater levels (red area) to moderate values of groundwater level (yellow area), to high values of groundwater level (blue area) on the map of the Gaza Strip. The coast of Rafah governorate (in the south of the Gaza Strip) has very low groundwater levels, while the east of Khan Younis governorate has very high groundwater levels. Such predictations will be helpful for the decision makers in planning the water resource use in the Gaza Strip. The following subsection will detect suspected outliers that may affect the predictions.

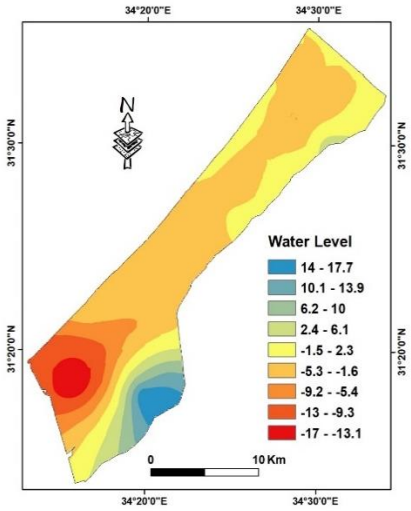

Figure 3. Predicted levels of the groundwater level based on ordinary kriging interpolation with an exponential variogram.

4.3 Outlier detection methods

We applied the considered outlier detection methods in geostatistical analysis for exponential variogram model. The associated cut-off points of the exponential variogram model for SIF, AND kriging, and IRF methods are 1175.502, 8.391 and 16.11, respectively. Table 4 lists the values of SIF, AND kriging and IRF for suspected outliers associated with measured water levels (WL), where the values that exceed the associated cut-off points are listed.

SIF has identified five wells as outliers, and the AND kriging has identified six wells as outliers, while IRF has identified only three wells as outliers.

There are two wells, numbers 77 and 80, identified as outliers by all of the three methods, with groundwater levels 20.14 and 17.32, respectively. Furthermore, wells 78 and 79 have been identified as outliers by SIF and kriging. All these four wells are located in the east of Khanyounis governorate (Fukhary area), where the groundwater level is about 11.8 m above sea level and this area is characterized by low saturated thickness. Furthermore, there is an artificial recharge of treated wastewater to the aquifer that infiltrate about 12,000, and leads to groundwater at more than 11 meters above the mean sea level (Aish, 2014).

The minimum water level is -20.00 in Rafah, which is a highly populated area with small number of wells: therefore the water abstraction from the wells is the greatest.

5. Conclusions

This article has considered the problem of outlier detection in univariate geostatistical data. The cut-off points of three methods were obtained and their performances were

Table 4. The detected outliers in geostatistical analysis

ID	Governorate	WL	SIF	Kriging	IRF
16	Khan Younis	9.69	-	10.57132	-
37	Khan Younis	12.56	-	31.96246	39043.30
40	Rafah	-20.00	1196.828	-	-
77	Khan Younis	20.14	1504.688	17.73483	86067.16
78	Khan Younis	18.88	1380.222	14.76079	-
79	Khan Younis	18.49	1343.658	13.82338	-
80	Khan Younis	17.32	1239.321	17.42490	56579.16

evaluated via a simulation. The methods were applied to groundwater level data for the Gaza coastal aquifer, where some outliers were detected and the discussion justified their identification.

Investigation should directed to multivariate outliers as well as to applying machine learning methods to outlier detection in geostatistical data.

References

Abuzaid, A. (2018). Evaluating spatial variability of groundwater electrical conductivity via geostatistical methods. *Journal of Al Azhar University-Gaza (Natural Sciences)*, *20*(2), 49-62.

Aish, A. (2014). Estimation of water balance components in the Gaza strip with GIS based wetspass model, *Civil and Environmental Research*, *6*(11), 77-84.

Aish A. Ayesh Kh. & Al-Najar H. (2021) Modelling of long-term effects of climate change on irrigation water requirement in the Gaza Strip, Palestine. *Arabian Journal of Geosciences*, *14*, 1-8.

Azevedo, L., Pereira, M. J., Ribeiro, M. C., & Soares, A. (2020). Geostatistical COVID-19 infection risk maps for Portugal. *International Journal of Health Geographics*, *19*(25), 1-8.

Ahmed, S. (2007). Application of Geostatistics in Hydrosciences. In M. Thangarajan (Eds.), *Groundwater*. Dordrecht, the Netherlands: Springer.

Bárdossy, A., & Kundzewicz, Z. W. (1990). Geostatistical methods for detection of outliers in groundwater quality spatial fields. *Journal of Hydrology, 115*(1-4), 343-359.

Barnett, V., & Lewis, T. (1994). *Outliers in statistical data* (3rd ed.). Chichesters, England: John Wiley & Sons.

Cuevas, A., Febrero, M., & Fraiman, R. (2007). Robust estimation and classification for functional data via projection-based depth notions. *Computational Statistics*, *22*(3), 481-496.

Chang, K.-T. (2006). *Introduction to geographic information systems*. Boston, MA: McGraw-Hill Higher Education.

Cooper, R. M., & Istok, J. D., (1988). Geostatistics applied to groundwater contamination. I. methodology. *Journal of Environmental Engineering, 114*, 270-285.

Delfiner, P. (1976). *Linear estimation of non stationary spatial phenomena Advanced geostatistics in the mining industry* (pp. 49-68). Dordrecht, the Netherlands: Springer.

Febrero, M., Galeano, P., & González-Manteiga, W. (2008). Outlier detection in functional data by depth measures, with application to identify abnormal NOx levels. *Environmetrics*, *19*(4), 331-345.

Gilbert, R. O. & Simpson, J. C. (1985) Kriging for estimating spatial pattern of contaminants: Potential and problems. *Environ Monit Assess*, *5*, 113–135.

Giraldo, R., Delicado, P., & Mateu, J. (2011). Ordinary kriging for function-valued spatial data. *Environmental and Ecological Statistics*, *18*(3), 411-426.

Hampel, F. R. (1974). The influence curve and its role in robust estimation. *Journal of the American Statistical Association*, *69*(346), 383-393.

Hayashi, K., Ishioka F., Ueda, T., Suito, H., & Kurihara, K. (2013). A detection of influential individuals for the risk prediction of endoleak formation after TEVAR based on a new framework of statistical sensitivity analysis. *Bulletin of the Computational Statistics of Japan* , *26*(2), 59–77.

Isaaks, E. H., & Srivastava, R. M. (1989). *An introduction to applied geostatistics*. Oxford, NY: Oxford University Press.

Isah, A. (2009). Spatio-temporal modeling of nonstationary processes, *Journal of Science, Education and Technology*, *2*(1), 372-377.

Lichtenstern, A. (2013). *Kriging methods in spatial statistics* (Master's thesis, Technical University of Munich, Germany).

Kim, S. (2014). Geostatistical data analysis with outlier detection. *Journal of the Korean Data Analysis Society*, *16*(5), 2285-2297.

Kim, M. G., & Jung, K. M. (2005). Detection of outliers in multivariate regression using plug-in method. *Journal of the Korean Data Analysis Society*, *7*(4), 1117-1124.

Kitanidis, P. K. (1983). Statistical estimation of polynomial generalized covariance functions and hydrologic applications. *Water Resecures Research*, *19*(4), 909-921.

Matheron, G. (1973). The intrinsic random functions and their applications. *Advances in Applied Probability*, 5(3), 439-468.

Nirel, R., Mugglestone, M. A., & Barnett, V. (1998). Outlier–robust spectral estimation for spatial lattice processes. *Communications in Statistics-Theory and Methods*, *27*(12), 3095-3111.

Olea, R. A. (2012). *Geostatistics for engineers and earth scientists*. New York, NY*:* Springer Science & Business Media,

Palestinian Central Bureau of Statistics, PCBS, (2020). *Palestine in figures 2019*. Ramallah, Palestine: Author.

Palestinian Water Authority, PWA (2010). *Setting-up groundwater protection plan of the coastal aquifer of Gaza strip*. PWA-WB-GEWP-01/ 09. Ramallah, Palestine: Author.

Palestinian Water Authority, PWA (2015). *Water resources status summary report/Gaza Strip*. Ramallah, Palestine: Author.

Romano, E., & Mateu, J. (2013). *Outlier detection for geostatistical functional data: an application to sensor data Classification and data mining* (pp. 131-138). Berlin, German: Springer.

Sun, M., Hou, E., Wu, J., Huang, J., Huang, X., & Xu, X. (2022). Spatial patterns and drivers of soil chemical properties in typical hickory plantations. *Forests*, *13*, 457.

United Nations Children's Fund, UNICEF (2018). Increasing water security in Gaza through seawater desalination. Document No: WASH/FN/12/2018

Vieira, R. J., Hartfield, L. J., Nielsen, D. R., & Biggar, W. J. (1982). Geostatistical theory and application to variability of some agronomical properties. *Hilgardia*, *51*(3), 1-75.

Yoo, S. M., & Um, I. H. (1999). On the estimation of semivariogram and spatial outliers with rainfall intensity data. *The Korean Journal of Applied Statistics*, *12*(1), 125-141.